Development and Field Testing of PTO Control Strategies for Two-Body Flexibly-Connected WECs

Brian Rosenberg*, Tim Mundon
Oscilla Power, Inc.
Seattle, WA, USA

Rob Cavagnaro, Curtis Rusch, Ben Maurer, Jim Thomson, Brian Polagye
University of Washington
Seattle, WA, USA

*Corresponding author: rosenberg@oscillapower.com

1. INTRODUCTION

Active control is the process of applying loads to a wave energy converter (WEC), typically through the power take-out system (PTO), such that the WEC's phase response is improved and power capture is increased. This technique has been studied extensively [1], particularly for single-body systems reacting against a fixed reference, and has shown potential for significant performance increases in controlled conditions [2]. The application of active control to two-body, self-referenced WECs has received some attention, however, uncertainty about the achievable performance gains remains.

A class of WEC showing significant recent interest is the two-body flexibly-connected point absorber, examples shown in figure 1. There are significant advantages to having a flexible tether connection between a surface float and a submerged reaction structure. These include greater simplicity of installation and reduction of structural cost, amongst others. Additionally, in the configuration used for Triton, the use of multiple tethers enables multi-mode energy capture. However, the application of active control techniques to flexibly-connected two-body WECs has received little to no attention in the literature.

The aim of this work is to evaluate different control strategies applied to a simple two-body single-tether architecture. The investigation will further attempt to tradeoff the benefits and feasibility of using control schemes relying on wave prediction techniques against causal methods. As a means of validating the identified strategies, these strategies will be tested and validated in the field using the single-tether MiniWEC test platform. Solutions for the single-tether system will then be adapted to the multiple-tether Triton WEC.

2. NUMERICAL MODEL

The MiniWEC is a two-body WEC platform developed at the University of Washington Applied Physics Lab (UW-APL) [3]. The WEC comprises a 1.8m diameter surface float and a 1.5m diameter heave plate that

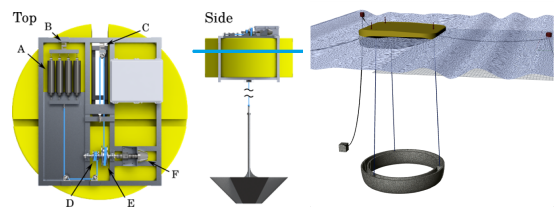

Figure 1: Two-body flexibly-connected WECs. MiniWEC (left). Triton (right).

hangs approximately 13m beneath the float. The power take-out (PTO) consists of a mechanical return spring, which supports the mean load of the heave plate, in parallel with a linear motor (LinMot), which captures power through the relative motion of the two bodies. In addition to resistive power capture, the LinMot can provide reactive (motoring) power flow, which is beneficial for some control strategies.

A time-domain numerical model of the MiniWEC was developed to evaluate the performance of different control strategies and to validate against experimental data collected in the field. This approach was selected in order to capture nonlinear effects, such as quadratic viscous drag, and to allow the investigation of discrete and nonlinear processes like PTO latching and slack tether events. The commercial hydrodynamic software Orcina Orcaflex was used to solve the equations of motion for the coupled marine and PTO systems.

Hydrodynamic properties for the float and heave plate were computed using the BEM code NEMOH. Results in heave are shown in figure 2. Plotted for the two bodies are the frequency-dependent added mass $A(\omega)$, radiation damping $B(\omega)$, and $H_e(i\omega)$, which is the transfer function between wave excitation force, F_e, and wave elevation, η. Inter-body hydrodynamic coupling between the two bodies for these properties is negligible due to several body lengths of separation.

For the surface float, Orcaflex handles the added mass and radiation terms through a Cummins decomposition

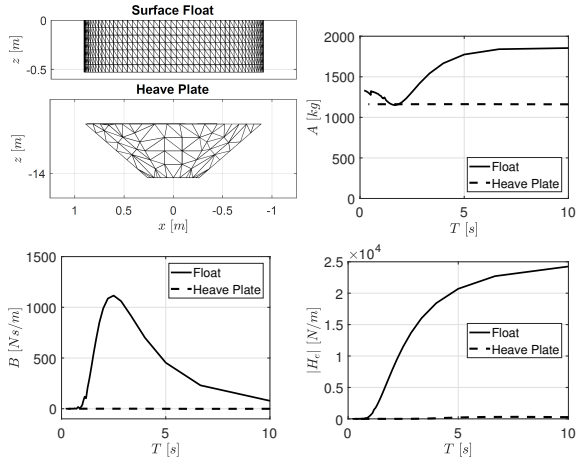

Figure 2: Mesh used for BEM solution (SWL @ $z = 0$) and hydrodynamic properties for the two bodies.

of the forces into an instantaneous added mass term and memory term expressed by a convolution product. Due to the large submergence depth of the heave plate (13m), it reacts minimally with the free surface and the hence wave radiation damping and wave excitation forces are negligible, as shown in figure 2. Additionally, its added mass becomes mostly frequency independent. As a result, the only hydrodynamic forces acting on the heave plate are the added mass and viscous drag and thus it can modeled using a simple Morison formulation. The drag coefficient on the heave plate was obtained from forced oscillation experiments [4], and the experimental and NEMOH results for added mass agree to within 10%. In the current model the heave plate added mass and drag coefficients are assumed to be constant, however they are somewhat sensitive to oscillation amplitude [5]. A slightly more accurate model, which will be the subject of future work, might allow the coefficients to vary with the local oscillation amplitude.

3. STRATEGIES INVESTIGATED

3.1 Passive Damping (PD)

Also sometimes known as optimal real control, the baseline control strategy is for the generator to behave as a linear passive damping element with a damping coefficient c_{gen}. Thus, the PTO force is given by:

$$f_{pto} = -c_{gen}(\dot{x}_1 - \dot{x}_2) - k_{mech}(x_1 - x_2) \qquad (1)$$

where x_1 and x_2 are the surface float and heave plate vertical displacements, respectively, and k_{mech} is the linear spring rate of the mechanical return spring.

3.2 Optimal Spring-Damping (OSD)

In this strategy, the generator has an additional spring component that acts in parallel with the mechanical return spring such that the effective spring rate of the PTO is the summation of the mechanical and generator spring rates. The generator spring component is energy neutral: energy is absorbed by the generator as it's moved away from its equilibrium position, and energy is reinjected back into the system as it moves back to its equilibrium position. The PTO force is given by:

$$f_{pto} = -c_{gen}(\dot{x}_1 - \dot{x}_2) - k_{eff}(x_1 - x_2) \qquad (2)$$

where $k_{eff} = k_{mech} + k_{gen}$.

3.3 Partial-Latching (PL)

Latching control involves locking the PTO at the extrema of displacement, where the velocity is zero, and releasing after an optimal time in order to force the device velocity to be in phase with the wave excitation force. Although latching is in practice suboptimal, significant gains in power have been realized for single-body point absorbers. The efficacy of latching applied to two-body WEC's has been questioned because the heave plate is not a perfectly stationary reaction structure, and the two bodies keep moving as one unit while latched. Nonetheless, recent work suggests latching control may provide some tangible power increases for two-body point absorbers [6]. For latching control, the PTO force is given by:

$$f_{pto} = -c_{gen}(\dot{x}_1 - \dot{x}_2) - f_{brake} \qquad (3)$$

where f_{brake} is the force needed to prevent relative motion between the two bodies.

While prior work has been conducted on rigidly connected two-body WECs, we will explore latching control subject to the constraints of a flexible connection, principally by applying the restriction that the tether should always remain taut. We therefore propose a 'partial-latching' strategy whereby the PTO is locked only after motion in one direction of travel, the upstroke. Practically, this means the two bodies are locked when there is zero relative motion and their separation distance is a local minimum. In the OrcaFlex model, this is implemented by engaging a PID position controller for the prescribed latch time when these conditions are achieved. For the MiniWEC field tests, this braking force is emulated in a similar way using the LinMot.

3.4 Complex-Conjugate (CC) Control

From linear frequency domain analysis, maximum power is absorbed when:

$$v_{r,opt} = \frac{F_o(i\omega)}{2R_i(\omega)} \qquad (4)$$

where $v_{r,opt}$ is the optimal PTO velocity [2]. For a single-body ground-referenced WEC, $F_o = F_e$, which leads to the well-known result that the PTO velocity should be in phase with the wave excitation force. For the two-body problem, $F_o = \frac{F_{e1}(i\omega)Z_2(i\omega)}{Z_1(i\omega)+Z_2(i\omega)}$, where Z_1 and Z_2 are the mechanical impedances for the float and heave plate, respectively, $Z_i = \frac{Z_1 Z_2}{Z_1+Z_2}$ is the two-body intrinsic impedance, and R_i is the real component of Z_i [7]. These terms are functions of the WEC's inherent hydrodynamic (figure 2) and hydrostatic properties. As CC is a linear approach, the heave plate quadratic drag term is approximated using a linearized drag coefficient, which is expected to be acceptable because the added mass forces tend to dominate over drag forces.

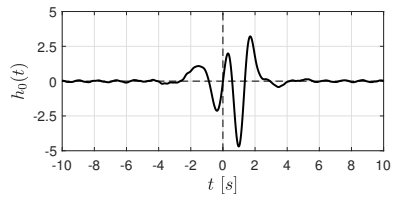

Figure 3: MiniWEC impulse response, h_o.

Using the convolution theorem:

$$v_{r,opt}(t) = \int_{-\infty}^{\infty} h_o(\tau)\eta(x; t-\tau)d\tau \tag{5}$$

where $h_o(t) = \mathcal{F}^{-1}\left[\frac{H_{e1}Z_2}{2R_i[Z_1+Z_2]}\right]$. $h_o(t)$ for the MiniWEC is shown in figure 3, demonstrating the noncausal behavior ($h_o(t)$ is nonzero for $t < 0$), however, the plot suggests that $\sim$ 4s of future wave knowledge is sufficient. The wave elevation η over this convolution interval may be calculated using an upwave measurement and a propagation model as discussed Section 4. In the OrcaFlex numerical model, CC control is implemented using a speed-controlled 'winch' element, which applies a force necessary to achieve $v_{r,opt}$ at each time step.

4. WAVE FORECASTING

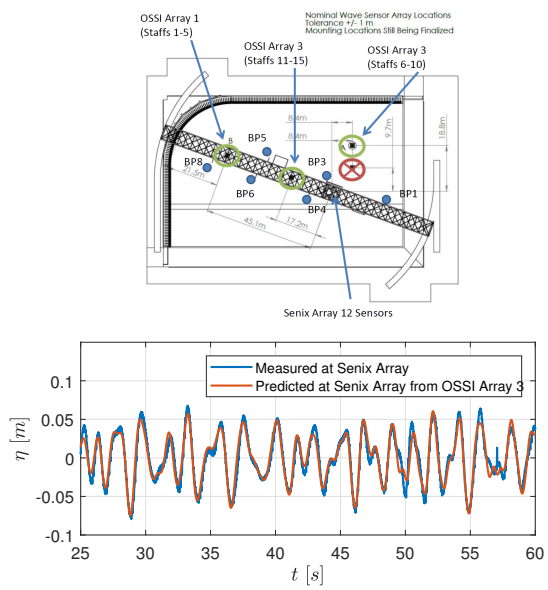

Figure 4: Wave probe arrays in the MASK basin, and wave forecasting for $T_p = 2.2$s, $H_s = 0.132$m.

The primary challenge with practically implementing CC control is that it requires knowledge of η at the location of the device up to some time in the future. Here, we consider 1-dimensional (long-crested) wave propagation from a probe upwave of the WEC.

In the frequency domain, the wave elevation profile at location x_B to relative to that at x_A, where the separation distance is d, is described by the transfer function $H_l(i\omega) = e^{-ik(\omega)d}$, where for deep water waves, the dispersion relation takes the form $k(\omega) = \omega^2/g$.

In the time domain, the wave profile at x_B can be expressed using the convolution theorem:

$$\eta(x_B; t) = \int_{-\infty}^{\infty} h_l(\tau)\eta(x_A; t-\tau)d\tau \tag{6}$$

where $h_l(t) = \mathcal{F}^{-1}[H_l(i\omega)]$ is the impulse response function that defines the linear propagation process in the time domain [2].

The accuracy and implementation of this model were investigated using the high-fidelity dataset measured for the DoE Wave Energy Prize [8]. Figure 4 shows the wave elevation measured by a probe in the 'Senix Array' compared to the wave elevation predicted there by an upwave probe in'OSSI Array 3' (the wave propagation direction was in line with these probes). The propagation model yields a good prediction with $(1-NRMSE)$ approaching 0.8.

5. RESULTS AND DISCUSSION

Numerical simulations of the MiniWEC were run over a range of wave periods typical of the Lake Washington and the Puget sound, $T_p = 2-6$s. Figure 5 shows how the mean power $\bar{P}$ varies with different PTO stiffness, k_{eff}, and damping, c_{gen}. The two contour plots shown correspond to $T_p = 2$s and 4s, both at $H_s = 0.1m$ using a Bretschneider wave spectrum. The time step was 0.01s with a simulation duration of 1800s.

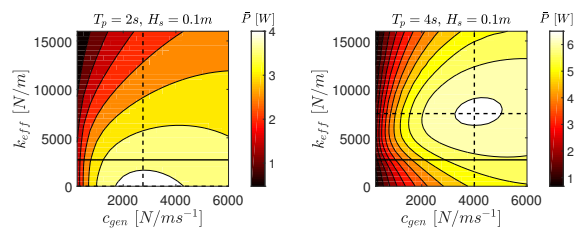

Figure 5: Average power in irregular waves ($T_p = [2, 4]$s, $H_s = 0.1$m) over a range of c_{gen} and k_{eff}. (–) k_{mech}. (- -) optimal c_{gen} and k_{eff}.

The solid horizontal line in figure 5 corresponds to k_{mech}. For PD control, the PTO can move anywhere along this line, and there is an optimal c_{gen} that maximizes power. Clearly, there is an advantage to OSD control as it allows the PTO to steer anywhere in the contour. In some cases (e.g. $T_p = 4s$) it is beneficial for k_{gen} to work in the same direction as the mechanical spring to create a stiffer k_{eff}, whereas in some cases (e.g. $T_p = 2s$) it is beneficial for k_{gen} to be negative, creating a softer k_{eff}. In practice, associated efficiency loss during generator 'motoring' should be considered as this will subtract from any performance gains for OSD relative to PD control. Alternatively, OSD control may be implemented by using a variable return spring system rather than a fixed spring, such as the hydropneumatic system proposed in [9].

Although not shown here for brevity, preliminary power comparisons between partial-latching and PD control in *monochromatic* waves demonstrate an approximately

15% power increase for PL over optimal PD. This power increase is consistent with the modest performance gains for two-body latching reported by [6]. Current work is aimed at further evaluating this approach, in addition to CC control, in irregular waves.

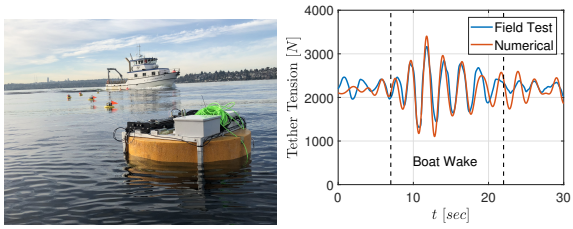

Figure 6: Excitation of SWIFT drifters and MiniWEC using a boat wake.

Shakedown tests of the MiniWEC were conducted in Lake Washington by hitting the WEC with a boat wake, which excites the WEC for 5-6 cycles (figure 6). Wave elevation of the boat wake was measured by an array of 4 SWIFT buoys [10], which were strung out in a line upwave of the MiniWEC. Preliminary comparisons of numerical model against the field data were performed by simulating the measured wave profile in the numerical model. A comparison of the experimental versus numerical tether tension fluctuations during a wave train is shown in figure 6, demonstrating decent agreement. It should be noted that the wave profiles measured by the SWIFTs outside of the 'boat wake' bands were only slightly above the noise floor, and any comparison here should be taken cautiously.

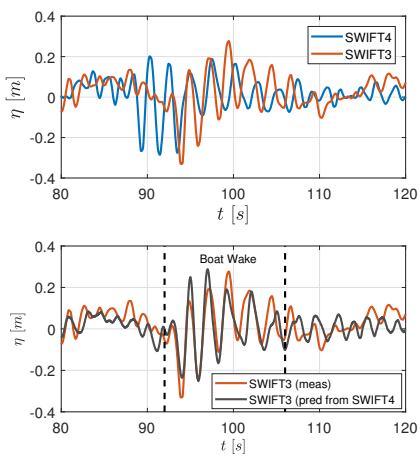

Figure 7: Wave forecasting using SWIFT measurements.

Furthermore, the wave propagation model described in Section 4 was used to assess the accuracy of wave forecasting between two SWIFT buoys. The onboard GPS measurements were used to estimate the SWIFT separation distance, d, and figure 7 compares the wave elevation measured at one buoy compared to the profile predicted by an upwave buoy. This approach works decently because the boat wakes are fairly long-crested. It is expected that forecast accuracy will deteriorate in short-crested waves, and this will be discussed further. A more sophisticated 2-dimensional forecasting model that accounts for wave spreading might be needed.

While the field data presented here are limited to boat wake excitation tests, deployments in energetic natural wave conditions in Lake Washington and Puget Sound are planned for January 2018.

6. ACKNOWLEDGEMENTS

This research was supported by the US Department of Defense Naval Facilities Engineering Command. The authors gratefully acknowledge assistance from individuals at UW-APL and UW.

7. REFERENCES

[1] Ringwood, J. V., Bacelli, G., and Fusco, F., 2014. "Energy-maximizing control of wave-energy converters: The development of control system technology to optimize their operation". *IEEE Control Systems,* ***34***(5), pp. 30–55.

[2] Korde, U. A., and Ringwood, J. V., 2016. *Hydrodynamic Control of Wave Energy Devices.* Cambridge University Press.

[3] Brown, A. C., and Thomson, J., 2016. "Phase-resolved heave plate dynamics for wave energy converters". In 4th Marine Energy Technology Symposium.

[4] Rusch, C. J., Maurer, B., Mundon, T. R., Stewart, A., and Polagye, B., 2017. "Hydrodynamics and scaling of heave plates for point absorbing wave energy converters". In European Wave and Tidal Energy Conference.

[5] Mundon, T. R., Rosenberg, B., and Van Rij, J., 2017. "Reaction body hydrodynamics for a multi-dof point absorbing wec". In Proceedings of the 12th European Wave and Tidal Energy Conference.

[6] Henriques, J., Lopes, M., Gomes, R., Gato, L., and Falcao, A., 2012. "On the annual wave energy absorption by two-body heaving wecs with latching control". *Renewable Energy,* ***45***, pp. 31–40.

[7] Falnes, J., 1999. "Wave-energy conversion through relative motion between two single-mode oscillating bodies". *Journal of Offshore Mechanics and Arctic Engineering.*

[8] Driscoll, F., Fingersh, L., Weber, J., Gunawan, B., Ruehl, K., Bull, D., Dallman, A., Newborn, D., Quintero, M., LaBonte, A., and Karwat, D., 2017. "Wave Energy Prize testing and data analysis overview". In 5th Marine Energy Technology Symposium.

[9] Mundon, T. R., Rosenberg, B., and Vining, J., 2017. "A hybrid drivedrive for low-speed, linear WEC applications". In 5th Marine Energy Technology Symposium.

[10] Thomson, J., 2012. "Wave breaking dissipation observed with 'SWIFT' drifters". *Journal of Atmospheric and Oceanic Technology,* ***29***(12), pp. 1866–1882.